

MODELLING AND SIMULATION OF THE CUTTING FORCES FOR 2.5 D POCKETS MACHINING

Ammar, A. A.; Bouaziz, Z.; Zghal, A.

Unit of Mechanics, Solids, Structures and Technological Development,
Ecole Supérieure des Sciences et Techniques de Tunis, B.P. 56. Bab Menara 1008 Tunis
Tunisia

Abstract:

The milling operation is a fundamental machining operation in industrial for the production of mechanical parts and injection moulds. During the machining of complex shapes, the tool engagement varies all along its path. The variation of the tool engagements leads automatically and inevitably to a corresponding variation of the cutting force. The objective of this article is to propose a cutting forces model in 2D milling pockets which takes into consideration the variation of the tool radial depth of cut. The machining simulation is applied onto a complex pocket through several different machining strategies in order to determine the cutting force variation and choose the adequate machining strategy.

Key Words: Milling 2.5D, Cutting Forces, Radial Depth of Cut

1. INTRODUCTION

The tool radial depth of cut is the value which describes which part of the tool is really involved in the machining, at a given time and position. During the milling of complex shapes, only a part of the tool is engaged in the material. The engagement of the tool varies all along the cutting path [1, 2]. This engagement variation has, as a consequence, a variation of the cutting forces. In this way, the controlling of the force and its direction permits to avoid the tool breakage and the damage of the machined part surface. We seek, then, to maintain the section of the chip that is the most constant possible. This means the conservation of regular and constant engagements of the tool. By controlling the tool engagement, we can supervise and control the cutting forces variations and consequently choose the machining strategy which guarantees the most possible continuous evolution of the mechanical demands applied onto the whole of the tool-material-machine set [3, 4]. It is then important to calculate, at each time, the radial depth of cut and relate the cutting forces to the tool path geometry. Several researchers have studied the variation effects of the radial depth of cut. Tsai et al. [5] have modified the tool path so as to keep the engagement angle, and therefore maintain the cutting force constant. Although their technique was good, it is difficult to see how it could be applied to the tool path for the complex geometries. Tarng and Shyr [6] have studied the effect of the radial depth of cut variation upon the cutting forces and they have adjusted the feed rate in such a way that the average cutting force remains constant for each value of the radial depth of cut. Their main objective was to avoid the machining instability. There is not any reference as to the way the cutting tool radial depth of cut has been calculated, or if its variation has been considered continuous or sampled. On the contrary, the work presented in this article shows in detail the approach and the procedure for the radial depth of cut quantification. In fact, two different approaches are possible for the determination of the tool engagement. The first type is based on the sampling discrete techniques. The second type, which is the approach adopted in our work, is based upon the analytic techniques and supplies the continuous functions of engagement [7, 8-10]. There are two main advantages in employing analytic techniques. First of all, some functions can be extracted to determine the cutting tool engagement at any point all along the tool path, without explicitly resolving any expensive Boolean operations. The second advantage is that because it is not based on sampling, it is more accurate than the sampling techniques. In this article, the quantification

model of the tool radial depth of cut is coupled with a cutting forces model [11-14] in milling 2D pockets, so as to simulate the cutting forces by taking account at the same time of the tool engagement variation and consequently of the tool path geometry.

2. CUTTING FORCES MODELLING

The cutting forces modelling allows the predicting of the forces without the settling of the real machining. It requires the knowledge of geometry of the tool, of the part, as well as of the cutting conditions. Figure 1 shows a tool at the time of machining in concordance and permanent regime. In comparison to this illustration, the forces model, developed in this paper, enables us to calculate at each time the cutting forces applied to the cutting edges engaged in the material. For a given angular position Φ , the tool is engaged in the material with a certain cutting thickness. It is the evaluation of the chip thickness which allows to calculate the cutting forces by means of a cutting specific pressure notion.

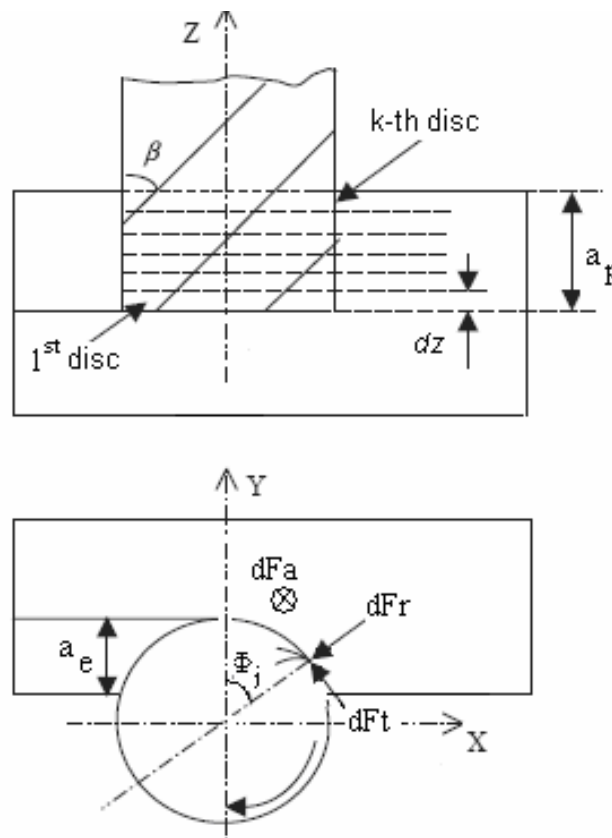


Figure 1: Cutting forces modelling.

2.1 Calculation of the chip instantaneous thickness

In milling, the instantaneous chip thickness varies according to the tool angular position. The discretization of the tool following the tool axis z and following some angular sectors around this same axis, allows to present the position of the tooth engaged in the workpiece and to deduce the chip instantaneous thickness relative to each position (Figure 2).

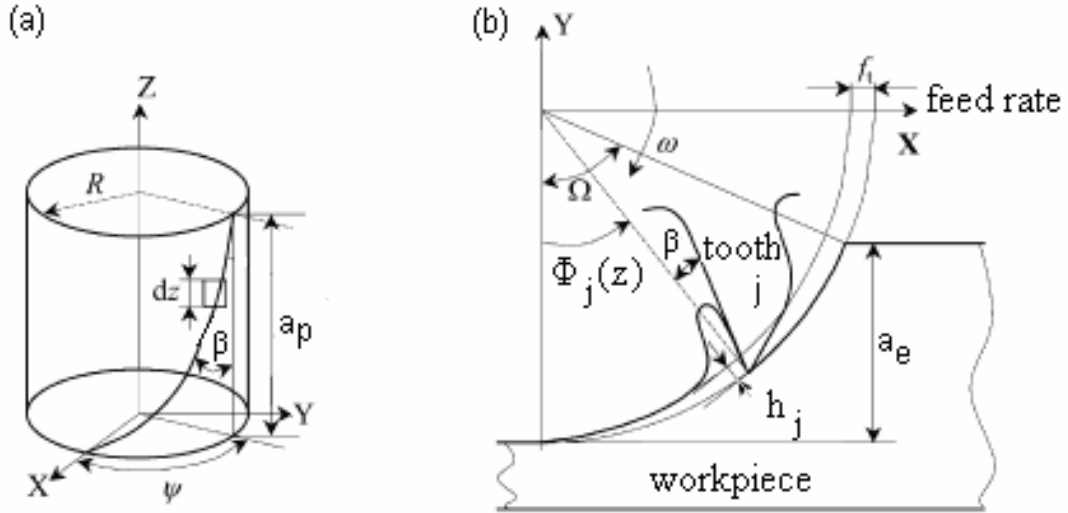


Figure 2: Variation of the cutting instantaneous thickness.

The chip instantaneous thickness can be calculated as follows:

$$h_j(\Phi, z) = f_t \sin \Phi_j(z) \quad (1)$$

Here, f_t is the feed rate per tooth, and $\Phi_j(z)$ is the angular position in comparison to the axis Y of the j -th tooth corresponding to the axial position z . Its value changes all along the axial direction as follows:

$$\Phi_j(z) = \Phi + (j-1)\Phi_p - \frac{\tan \beta}{R} z \quad j = 1, \dots, N_D \quad (2)$$

Φ_p is the angle between two consecutive teeth such as $\Phi_p = \frac{2\pi}{N_D}$, where, N_D is the number of teeth and R is the tool radius.

The part of tool engaged in the workpiece is discretized in N_z disc, following the axis z . We note $z(k)$ the position of the average surface of the k -th elementary disc dz :

$$z(k) = (k-1)dz + \frac{dz}{2} \quad k=1, \dots, N_z \quad (3)$$

Hence, equation 2 can be re-written in the following way:

$$\Phi_j(z) = \Phi + (j-1)\Phi_p - \left((k-1)dz + \frac{dz}{2}\right) \frac{\tan \beta}{R} \quad (4)$$

If $\varphi_e \leq \Phi_j(z) \leq \varphi_s$, then it has a value, otherwise it is null. φ_e is the position at the moment when the tool tooth gets into the workpiece for machining and φ_s is the angular position at the moment when the tooth of the tool gets out of the workpiece to machine. The angle between the entry of the tooth φ_e and the exit of the tooth φ_s is called the engagement angle, noted ϕ_{eng} , and which can be written as follows:

$$\phi_{eng} = \arccos\left(1 - \frac{a_e}{R}\right) \quad (5)$$

Where a_e is the cutting tool radial depth of cut.

2.2 Formulation of the cutting forces model

The forces model, we have presented, consists in characterising the cutting force for a tool-materials couple, with the help of a specific coefficient called cutting specific pressure. The latter puts into evidence a proportion relation between the cutting forces and the chip section. The tangential cutting force dF_t , radial cutting force dF_r and axial cutting force dF_a applied onto the tooth j at the level of the elementary disc k , can be written as follows:

$$\begin{cases} dF_t(\Phi, j, k) = K_t h_j(\Phi, z) dz, \\ dF_r(\Phi, j, k) = K_r dF_t(\Phi, j, k), \\ dF_a(\Phi, j, k) = K_a dF_t(\Phi, j, k), \end{cases} \quad (6)$$

The coefficients K_t , K_r et K_a are the specific cutting force coefficients for each tangential, radial and axial direction. The determining of these coefficients is based on the forces experimental measurements which necessitate a certain number of preliminary experiments. Following the axis X, Y, Z, the elementary forces applied onto the elementary disc are determined by summation on the teeth in contact with the material:

$$\begin{cases} dF_x(\Phi, k) = \sum_{j=1}^{N_D} \{ dF_r(\Phi, j, k) \sin \Phi_j(z) + dF_t(\Phi, j, k) \cos \Phi_j(z) \} \\ dF_y(\Phi, k) = \sum_{j=1}^{N_D} \{ dF_r(\Phi, j, k) \cos \Phi_j(z) + dF_t(\Phi, j, k) \sin \Phi_j(z) \} \\ dF_z(\Phi, k) = \sum_{j=1}^{N_D} dF_a(\Phi, j, k) \end{cases} \quad (7)$$

The resultant of the cutting forces is obtained by summation on all the elementary discs:

$$\begin{cases} F_x(\Phi) = \sum_{k=1}^{N_Z} dF_x(\Phi, k) \\ F_y(\Phi) = \sum_{k=1}^{N_Z} dF_y(\Phi, k) \\ F_z(\Phi) = \sum_{k=1}^{N_Z} dF_z(\Phi, k) \end{cases} \quad (8)$$

By integrating the equation 6 and 7 in the equation 8, we obtain:

$$\begin{cases} F_x(\Phi) = \sum_{k=1}^{N_z} \sum_{j=1}^{N_D} K_t \cdot dz \cdot f_t \left\{ \cos \Phi_j(z) \sin \Phi_j(z) - K_r \sin^2 \Phi_j(z) \right\} \\ F_y(\Phi) = \sum_{k=1}^{N_z} \sum_{j=1}^{N_D} K_t \cdot dz \cdot f_t \left\{ K_r \sin \Phi_j(z) \cos \Phi_j(z) + \sin^2 \Phi_j(z) \right\} \\ F_z(\Phi) = \sum_{k=1}^{N_z} \sum_{j=1}^{N_D} K_t \cdot K_a \cdot f_t \cdot \sin \Phi_j(z) dz \end{cases} \quad (9)$$

3. THE RADIAL DEPTH OF CUT a_e MODELLING

To try to quantify the influence of the machining path upon the cutting forces evolution is one of the tasks of this work. The calculation of the tool axial and radial depth of cut allows at any time to relate the cutting forces to the tool path geometry. In the case of the pocket machining, the axial engagement is constant. On the contrary, the radial depth of cut varies all along the machining path.

Figure 3 presents the tool path in the case of a spiral out machining with a tool $D=20$ mm in diameter. We note, indeed, that even for this simple rectangular pocket, there is a considerable variation of the radial depth of cut. In fact, the tool starts the machining of 1 to 2, with a constant and maximal engagement, equal to the tool diameter. Then, the radial depth of cut varies and more particularly where there is a changing of direction. Figure 4 presents the tool path of 2 to 3 and of 3 to 4 as well as the variation of the radial depth of cut in that area. The radial depth of cut increases when the tool moves away from 2, and when it is at a distance of $D/2$ of 2, it reaches its maximum, which is equal to the tool diameter. After that, the radial depth of cut undergoes a slight variation, and then it remains constant at a value of 75% of the tool diameter for the most part of the path between 3 and 4.

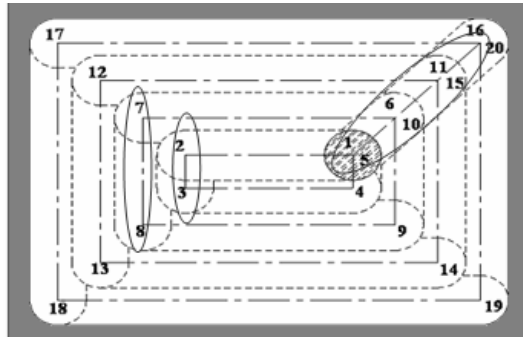


Figure 3: Spiral out machining.

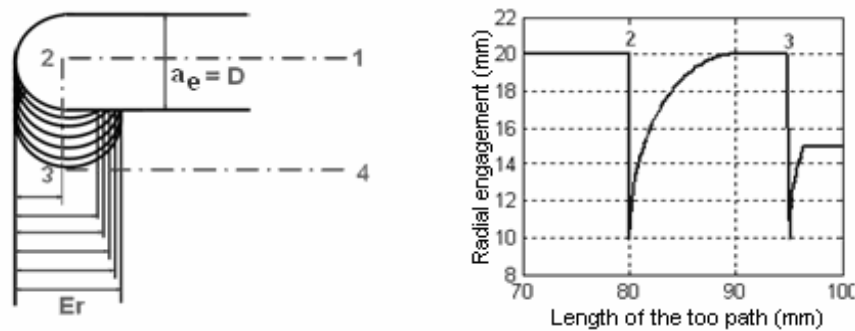


Figure 4: Radial depth of cut variation at the time of the changing direction of 90°.

To make it possible to quantify the radial depth of cut variation at any point of the machining path, our approach has been conceived in three steps, namely:

Step 1: Calculation of the pocket hollowing out path

The calculation of the path of a pocket hollowing out has for data the geometry of the pocket (borders, bottom, top ...) and the cutting conditions (feed rate, machining strategy, axial pass, radial pass...). Since this calculation is not simple, we must inevitably have recourse to an algorithm of a path geometry generation. In our case, the generation of a pocket hollowing out path is realized in an almost automatic way with the help of software Master Cam. This latter provides us with all the necessary information about the geometry of the tool path as well as the coordinates of all the points situated on this path.

Step 2: Tool path discretization

The path obtained by the CAM is generally complex and has a considerable number of direction changings because the pocket is a closed space. To make it possible to quantify the radial depth of cut variation of the tool, at any point of the path, it is necessary to have recourse to the tool path discretization in different zones, namely:

- Zones for which the radial depth of cut remains constant
- Zones for which the radial depth of cut undergoes a variation. These variations are situated mainly in the corners and at any change of the machining direction.

Step 3: Calculation of the radial depth of cut

The method adopted for the calculation of the tool radial depth of cut is a geometric method. Its principle is to determine an analytic expression of the tool radial depth of cut for a given machining strategy at any point of the cutting tool path. The implementation of these expressions in the software MATLAB, allows simulating the radial depth of cut according to the tool path length.

By way of example, for passing from 2 to 3, the tool changes direction according to an angle of 90° . The radial depth of cut varies, and its variation depends on the radial depth, on the distance between the two points 2 and 3 and on the tool position all along the segment "2-3". Figure 5 presents the two possible cases as well as the analytic expressions of the radial depth of cut in this zone.

We note L_{2-3} the length of the segment "2-3" and d_2 the distance between the tool centre and point 2.

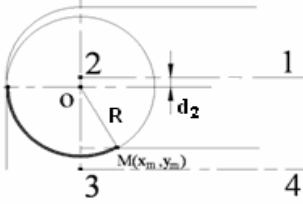
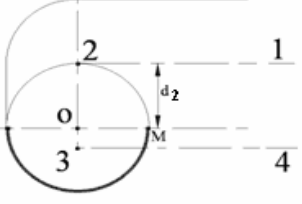
Case where $d_2 < R$	Case where $d_2 > R$
	
$a_{e_{2,3}} = R + \sqrt{d_2(2R - d_2)}$	$a_{e_{2,3}} = 2R$

Figure 5: Radial depth of cut of the tool in zone 2.

Other example of calculation is presented in Figure 6, which shows the variation of the radial depth of cut in the machining direction between 6 and 7. We notice that there are 4 different regions and consequently, it was necessary to establish, for each of them, the analytic expression of the radial depth of cut, namely:

1st region: the one before point M reaches point A

$$a_{e6,7} = R - \frac{\operatorname{tg}(\alpha)(\frac{r}{\sin(\alpha)} - d_6) - \operatorname{tg}(\alpha)\sqrt{R^2(tg^2(\alpha)+1) - \operatorname{tg}^2(\alpha)(\frac{r}{\sin\alpha} - d_6)^2}}{tg^2(\alpha)+1} \quad (10)$$

2nd region: for which point M belongs to the segment [AB]

$$a_{e_6 7} = R + (L_{5-6} \sin \alpha - R) \quad (11)$$

3rd region: for which point M belongs to the arc [BC]

$$a_{e_{6,7}} = R - \frac{1}{2}y_2 + \frac{x_2}{y_2} \frac{\sqrt{y_2^2(x_2^2 + y_2^2)(4r^2 - (x_2^2 + y_2^2))}}{2(x_2^2 + y_2^2)} \quad (12)$$

$$\text{Where } \begin{cases} x_2 = d_6(L_{1-2} + L_{5-6} \cos(\alpha)) \\ y_2 = -L_{5-6} \sin(\alpha) \end{cases} \quad (13)$$

4th region: the one after point M has outdone point C

$$a_{e67} = 2R \quad (14)$$

d_6 is the distance between the tool centre and point 6, L_{6-7} is the distance between point 6 and 7 and L_{5-6} is the distance between point 5 and 6.

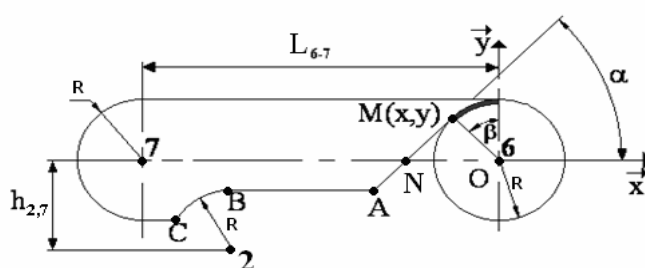


Figure 6: Passing of the tool from 6 to 7.

In our work, this procedure for the quantification of the tool radial depth of cut is adopted by the two machining strategies Zigzag and spiral-out.

4. NUMERICAL SIMULATIONS: COUPLING BETWEEN THE CUTTING FORCES MODEL AND THE RADIAL DEPTH OF CUT MODEL

In this part, we carry out the coupling of two models of cutting forces and of radial depth of cut, in order to simulate the cutting forces, taking into account the variation of the tool radial depth of cut.

4.1 Software implementation for the cutting forces calculation

In order to be able to simulate the cutting forces variation in milling, the model we have developed has been implemented under MATLAB. As a first step, the cutting coefficients K_t , K_r and K_a are supposed to be known. For our case, these coefficients are issued from the bibliography [15]. The algorithm developed for the cutting forces prediction and simulation can be written in the following organigram (Figure 7). For the input variable, we find the characteristic relative to the couple tool/material and the cutting conditions. For the output variable, we also find the values and variation of the cutting forces in each direction X, Y and Z.

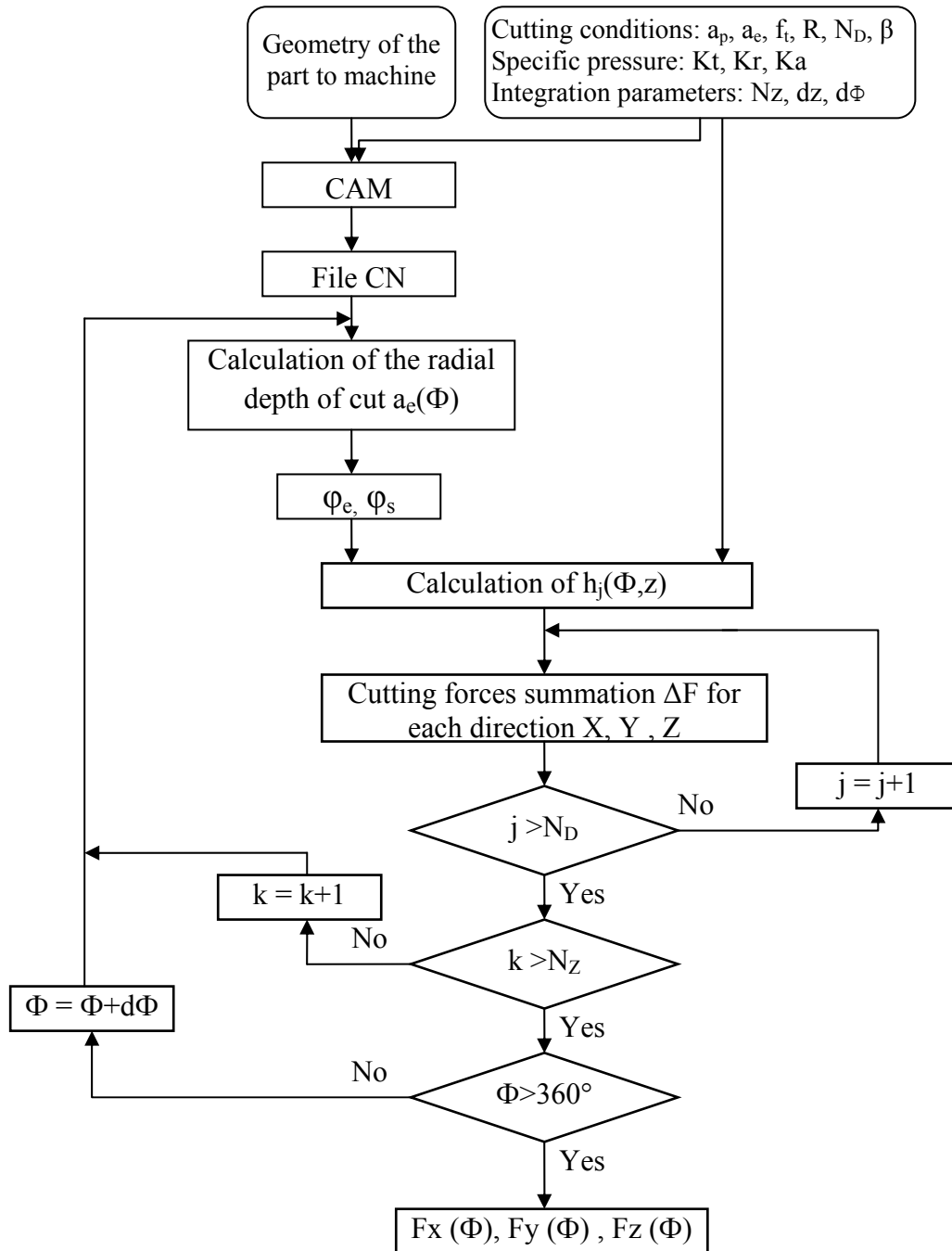


Figure 7: Algorithm of the cutting forces calculation.

4.2 Cutting conditions

The simulation of the forces is tackled for the pocket machining case by using two machining strategies zigzag and spiral out. For the two cases, we consider the same pocket and the same cutting conditions. The pocket we have studied is of a rectangular shape, its dimensions are given by Figure 8 and the cutting conditions are presented in Table I.

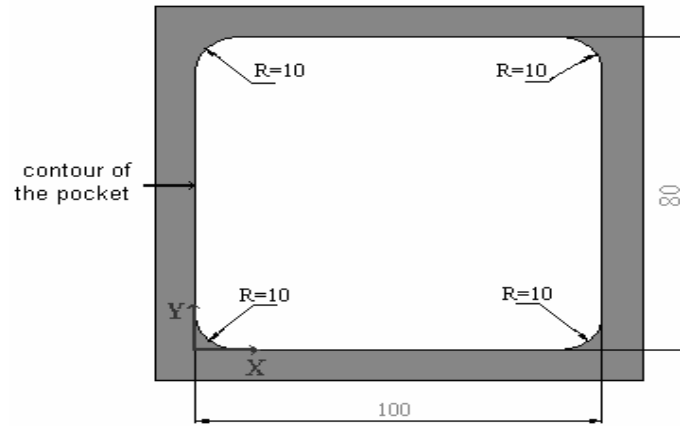


Figure 8: Presentation of the pocket under study.

Table I: Cutting conditions.

Tool	Two-sized monoblock carbide tool
Number of teeth (N_D)	$N_D=2$
Tool diameter (D)	D= 20 mm
Helix angle (β)	$\beta=40^\circ$
Machining material	X38Cr MoV5
Cutting speed	$V_c= 127$ m/min
Feed rate per tooth (f_t)	$f_t= 0.025$ mm/ tooth
Axial depth (a_p)	$a_p = 1$ mm
Radial depth	75% tool diameter

4.3 Zigzag machining

For the pocket we have studied, the trajectory generation is carried out by the software MASTER CAM. For this example, the machining strategy used is in zigzag. The pocket hollowing out path is given by Figure 9.

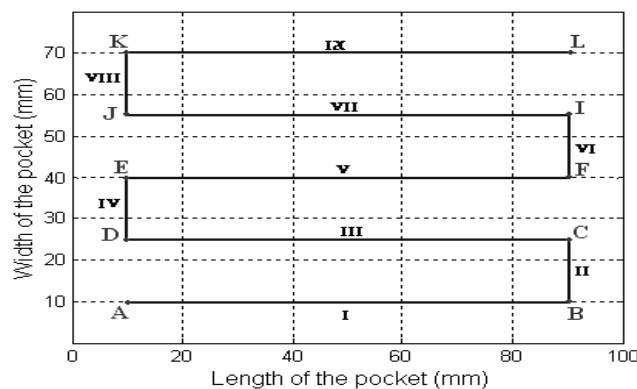


Figure 9: The tool path during the zigzag hollowing out of a pocket.

4.3.1 Simulation of the tool radial depth of cut

In order to simulate the radial depth of cut variation, we have implemented under MATLAB the calculation model of the tool engagement. We integrate, besides this model, all the informations about the geometry of the pocket and of the machining path as well as the coordinates of all the points situated on this path. For the case we have studied, the simulation of the radial depth of cut is given by Figure 10 on which the radial depth of cut is represented either according to the length of the tool path (Figure 10a), or directly on the tool path through segments of straight lines perpendicular to the machining path (Figure 10b).

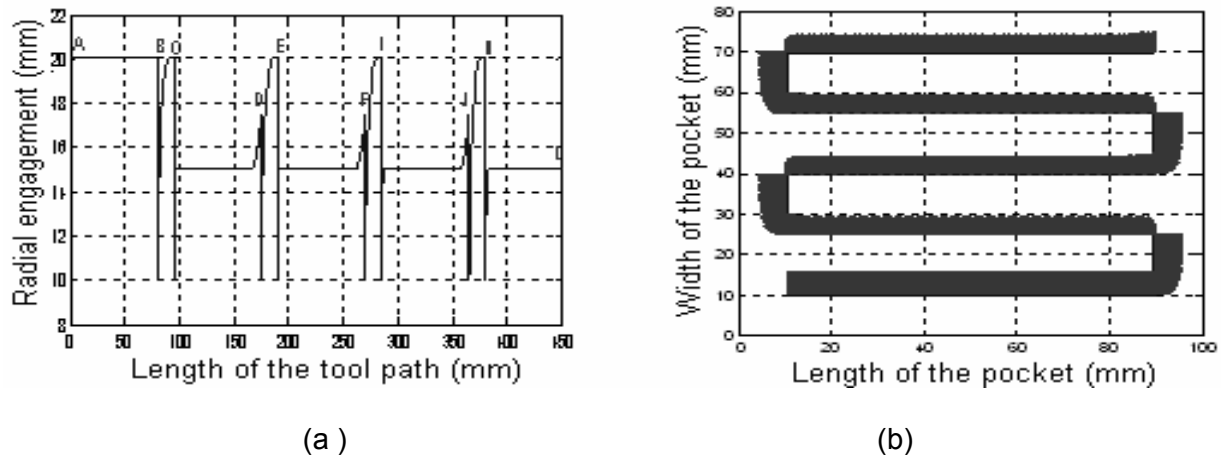


Figure 10: The simulation of the radial depth of cut for a zigzag machining strategy.

According to Figure 10a, we notice quite well that the tool starts the machining work from point A to point B with a maximal constant radial depth of cut corresponding to its diameter. From point B onwards, the cutting tool must change its direction to reach point C. In this zone (zone II), the tool radial depth of cut presents some disruption. For our case, the changing of direction is realized by right angles. Not only a jump results as a consequence (a fall of a maximal value from 20 mm to a value of 10 mm) but also a moment when the tool can machine the maximum of material (maximal engagement), even for a short distance, until point C. From point C to point D (Zone III), the radial depth of cut presents a weak variation, then it remains constant at a value equal to that of the radial depth (75% tool diameter). When it reaches point D, the cutting tool changes its direction to reach point E. The radial depth of cut undergoes some disruption, then, it becomes stable at the same departure value from point D (15 mm), the value with which the tool continues its path until point F. From point E, we have the same phenomenon again and again. In fact, the zones VI and VIII are similar to zone IV. Moreover, zones V, VII and IX are quite similar to zone III. The direct representation of the radial depth of cut on the tool path (Figure 10b) allows to give a general idea about the engagement evolution all along the tool path. We observe quite well some constant bands for which the radial depth of cut keeps the same value and we also observe some variable engagement bands corresponding to the zones of direction changing.

4.3.2 Cutting forces simulation

By coupling the two models of cutting forces and of radial depth of cut, it was possible to simulate the cutting forces by taking into account the radial depth of cut variation. The results of numerical simulation of the cutting forces, for the case of the hollowing out of the pocket we have studied, are represented in Figure 11. We have used then the strategy of zigzag machining.

The curves above (Figure 11) represent the cutting force components according to the time allowed for a machining strategy in zigzag. We can remark a good concordance

between the cutting forces variation and that of the tool radial depth of cut. In fact, for a maximal constant radial depth of cut, in zone I, the cutting force variation is maximal. It is also limited in a constant band. The disruption of the cutting forces components which appear in the zones II, IV, VI and VIII, correspond to the moments when the tool is no more in contact with the material and when the evolution of the tool radial depth of cut is discontinuous. For the zones III and VII, the variations of the cutting forces become stable but the force amplitude decreases in comparison with the zone I, especially for the components F_x and F_y . This decreasing is resulted from the decreasing of the radial depth of cut in these zones.

4.4 Spiral out machining

Next, we are about to simulate the variation of the tool radial depth of cut and the cutting forces for the case of a pocket hollowing out spiral. The path of the cutting tool given by the MASTER CAM software is represented in the following figure (Figure 12).

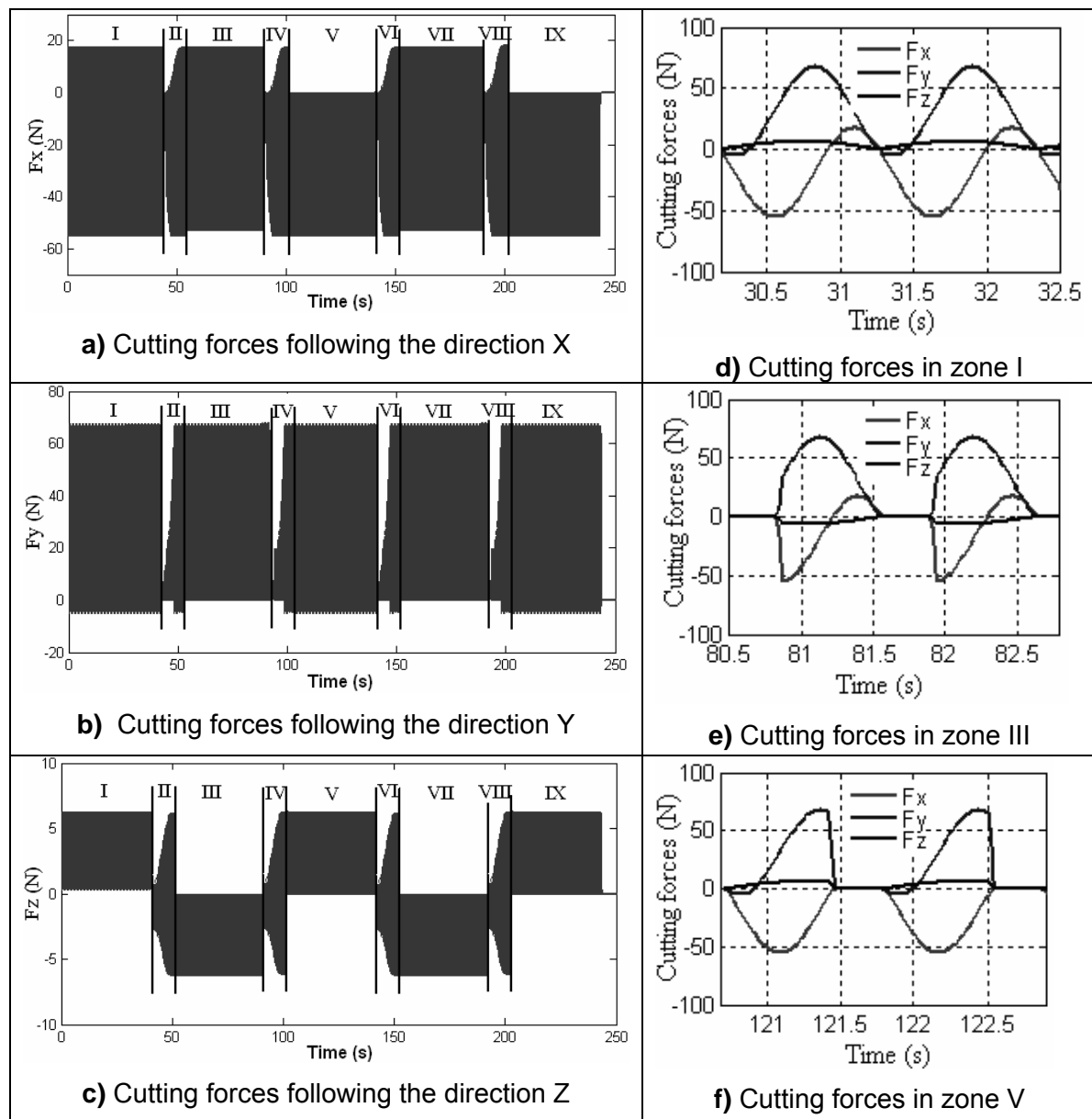


Figure 11: Cutting forces variation for the case of a pocket hollowing out in zigzag.

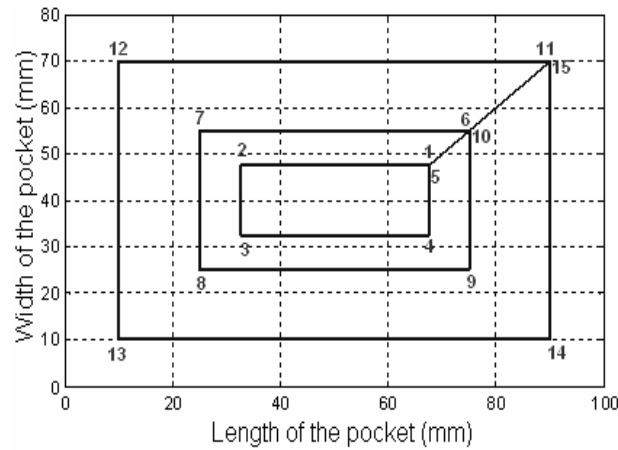


Figure 12: The tool path during the spiral hollowing out of a pocket.

4.4.1 Simulation of the radial depth of cut

Figure 13 shows the numerical simulation results of the tool radial depth of cut for the pocket we have studied by using the spiral machining strategy.

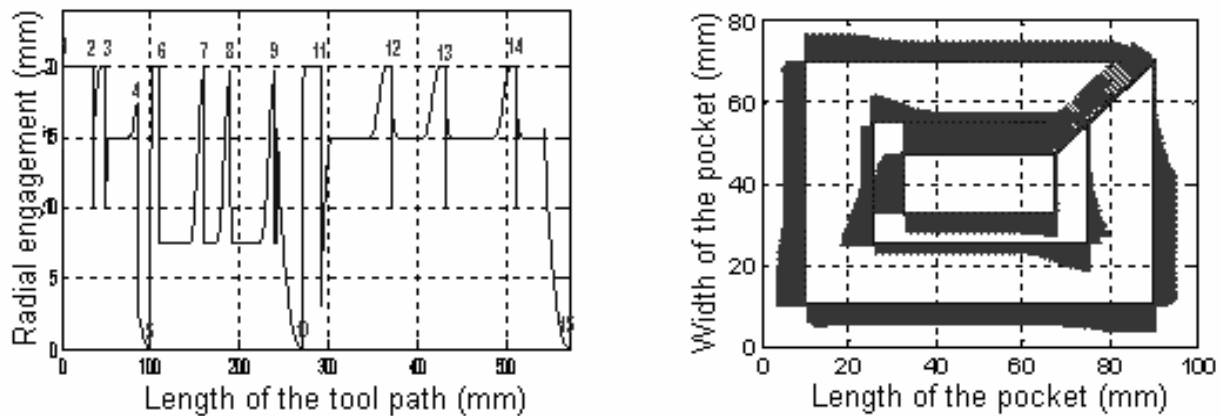


Figure 13: Radial depth of cut simulation for a spiral machining strategy.

Through observing the evolution of the tool radial depth of cut, all along the machining path, we find that the zone of passage from point 1 to point 2 has a constant maximal radial depth of cut which is equal to the cutting tool diameter. From point 2 onwards, the radial depth of cut presents some disruptions which generally correspond to the zones of direction changing.

4.4.2 Cutting forces simulation

The curves presented below Figure 14 show the cutting forces profile, in relation to the time for a spiral machining strategy. The bands are divided into zones according to the tool path.

We notice that the forces variation follows the tool radial depth of cut variation (Figure 14). In fact, for a constant radial depth of cut, the cutting force components vary in a constant band. Likewise, for a discontinuous radial depth of cut, the cutting forces undergo some disruptions, which occur mainly in the zones of direction changing.

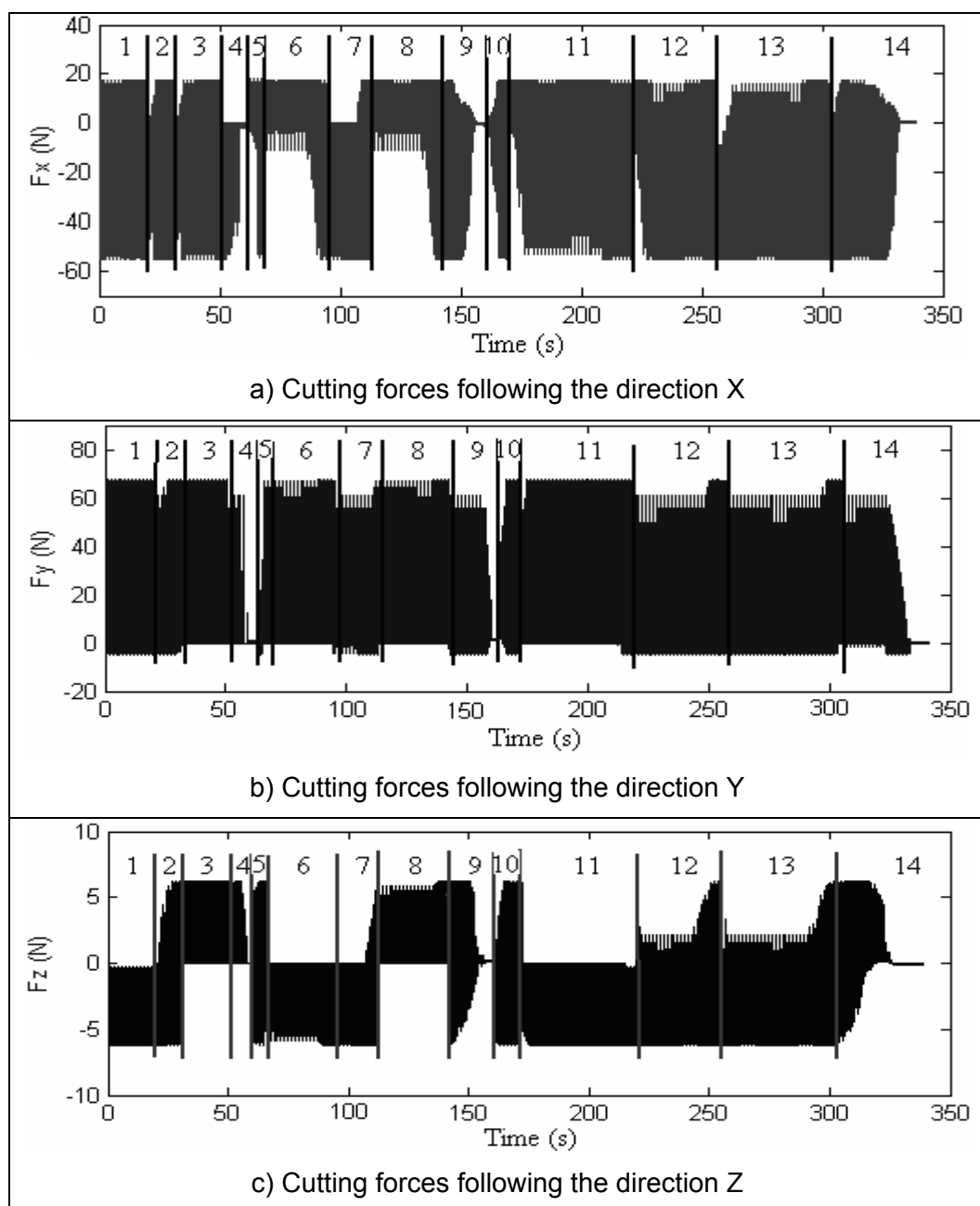


Figure 14: Cutting force variation for the case of a pocket spiral out hollowing.

5. CONCLUSION

In this article, we have carried out the coupling of two cutting forces models and the radial depth of cut in order to be able to simulate the cutting forces in milling 2.5 axes, taking account at the same time of the tool radial depth of cut variation. As application of this work, we have tackled the case of a rectangular pocket hollowing out, using the two strategies of zigzag and spiral out machining. Through analysing the numerical simulation results of the radial depth of cut and of the cutting forces, it is proved that the geometry of the path exerts an important influence upon the tool engagement and also upon the evolution of the mechanical actions applied onto the tool all along the path. Then, we have to choose the strategy which allows the most to guarantee a continuous evolution of the cutting forces. In our case, the zigzag machining strategy is the best for the hollowing out of the pocket we have studied.

REFERENCES

- [1] Hinduja, S.; Roaydi, A.; Philimis, P.; Barrow, G. (2001). Determination of optimum cutter diameter for machining 2 1/2-O pockerts, *International Journal of Machine Tools and Manufacture*, Vol. 41, pp. 687-702
- [2] Satyandra K. Gupta; Sunil K. Saini; Brent W. Spranklin; Zhiyang Y. (2005). Geometric algorithms for computing cutter engagement functions in 2.5 D milling operations, *Computer-Aided Design*, Vol. 37, pp. 1469-1480
- [3] Yao Z, Gupta SK. (2004). Cutter path generation for 2.5D milling by combining multiple different cutter path patterns. *International journal of production research*; 2141–61
- [4] Fussell B.K.; Jerard R.B.; Hemmett G. (2001). Robust feedrate selection for 3- Axis NC machining using discrete models. *Journal of manufacturing science and engineering*; 123:214–24
- [5] Tsai, M. D.; Takata, S.; Inui, M.; Kimura, F.; Sata, T. (1991). Operation planning based on cutting process models, *Annals of CIRP* 40 (1) 95–98
- [6] Tarng, Y. S.; Shyur, Y. Y. (1993). Identification of radial depth of cut in numerical control pocketing routines, *International Journal of Machine Tools & Manufacture*. 33 (1) 1–11
- [7] Spence, A.; Altintas, Y.; Kirkpatrick, D. (1990). Direct calculation of machining parameters from a solid model. *Computers in Industry*, 14: 271–80
- [8] Spence, A.; Altintas, Y. (1991). CAD assisted adaptive control for milling. *Journal of dynamic systems, measurement, and control*, 113: 444–50
- [9] Kramer T.R. (1992). Pocket milling with tool engagement detection. *Journal of Manufacturing Systems*; 11(2):114–23
- [10] Spence, A.; Abrari, F.; Elbestawi, A. (2000). Integrated solid modeller based solutions for machining. *Computer Aided Design*; 32:553–68
- [11] Ko, J. H.; Yun, W. S.; Cho, D. W.; Ehemann, K. F. (2002). Development of a Virtual Machining System. Part I: Approximation of the Size Effect for Cutting Force Prediction, *International Journal of Machine Tools and Manufacture*, Vol. 42, pp. 1595-1605
- [12] Yoon, M. C.; Kim, Y. G. (2004). Cutting dynamic force modelling of end milling operation, *International Journal of Machine Tools and Manufacture*, Vol. 155-156, pp.1383-1389
- [13] Budak, E. (2006). Analytical models for high performance milling. Part I: Cutting forces, structural deformations and tolerance integrity, *International Journal of Machine Tools and Manufacture*, Vol. 46, pp.1478-1488
- [14] Li, H. Z.; Zhang, W. B.; Li, X. P. (2001). Modelling of Cutting Forces en Helical End Milling Using a Predictive Machining Theory, *International Journal of Mechanical Sciences*, Vol. 43, pp. 1711-1730
- [15] Bissey-Breton, S. (2005). Développement d'un modèle d'efforts de coupe. Applications à des familles d'outils : cas du fraisage des aciers traités thermiquement, PhD thesis, ENSAM Paris, France